Excited-State Symmetry Breaking and Localization in a Noncentrosymmetric Electron Donor–Acceptor–Donor Molecule

Dereka, Bogdan; Balanikas, Vangelis; Rosspeintner, Arnulf; Li, Zhiquan; Liska, Robert; Vauthey, Eric

How to cite

DEREKA, Bogdan et al. Excited-State Symmetry Breaking and Localization in a Noncentrosymmetric Electron Donor–Acceptor–Donor Molecule. In: The journal of physical chemistry letters, 2024, vol. 15, p. 8280–8286. doi: 10.1021/acs.jpclett.4c01694

This publication URL: https://archive-ouverte.unige.ch/unige:179219
Publication DOI: 10.1021/acs.jpclett.4c01694

Excited-State Symmetry Breaking and Localisation in a Non-Centrosymmetric Electron Donor-Acceptor-Donor Molecule

Bogdan Dereka,*,† Evangelos Balanikas,‡ Arnulf Rosspeintner,‡ Zhiquan Li,¶,§ Robert Liska,¶ and Eric Vauthey*,‡

†*Department of Chemistry, University of Zurich, CH-8057 Zurich, Switzerland.*
‡*Department of Physical Chemistry, University of Geneva, CH-1211 Geneva, Switzerland.*
¶*Institute of Applied Synthetic Chemistry, Division of Macromolecular Chemistry, Vienna University of Technology, Getreidemarkt 9/163/MC, 1060 Vienna, Austria.*
§*Present address: Guandong University of Technology, School of Materials and Energy, 100, Waihuan West road, Guangzhou, Guangdong 510006, P.R.China.*

E-mail: bogdan.dereka@chem.uzh.ch; eric.vauthey@unige.ch

Abstract

Electronic excitation in quadrupolar conjugated molecules rapidly localises on a single electron donor-acceptor (DA) branch when in polar environments. The loss of centre of inversion upon this excited-state symmetry breaking (ES-SB) can be monitored by exploiting the relaxation of the exclusion rules for IR and Raman vibrational transitions. Here, we compare ES-SB in a right-angled (**1**) and a centrosymmetric (**2**) DAD dyes using time-resolved IR spectroscopy. We show that the localisation of the excitation can also be identified with the bent molecule **1**. We find that, contrary to dye **2**, subpopulations with localised and delocalised excitation coexist for **1** in weak to medium polar solvents. This difference originates from torsional disorder present in the excited state of **1** but not of **2**. Additionally, irreversible localisation in a bent molecule is shown to require higher solvent polarity than in a centrosymmetric one.

TOC Graphic

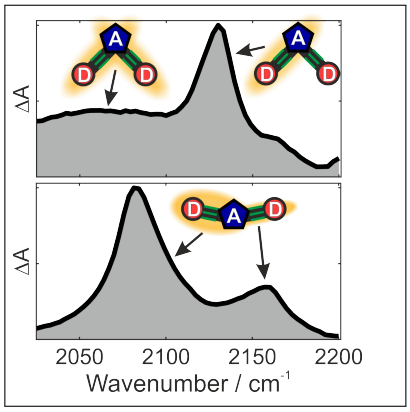

Over the past few years, excited-state symmetry breaking (ES-SB) was found to be rather common in quadrupolar conjugated molecules dissolved in polar media.[1–28] During this process, the electronic excitation, initially distributed evenly over the whole molecule, localises, at least partially, on one of the two electron donor-acceptor (DA) branches. As ES-SB confers a dipolar character to the excited state, its occurrence was first inferred from the fluorescence solvatochromism that was unexpectedly large for centrosymmetric molecules.[1–3,14–17,19,20,24] More recently, this phenomenon could be visualised in real time using time-resolved IR (TRIR) spectroscopy, by exploiting the breakdown of the exclusion rules for IR- and Raman-allowed vibrational transitions.[7,8,13,23,28] These two approaches work particularly well to detect ES-SB in centrosymmetric molecules because of the resulting loss of centre of inversion.

In principle, ES-SB should also occur in double-branched molecules of lower symmetry. However, its detection could be problematic because, first, fluorescence solvatochromism should be present even when excitation is delocalised evenly over the molecule and, second, the exclusion rule for vibrational transitions can no longer be exploited.

We report here on our investigation of the excited-state dynamics of a non-linear double-branched DAD dye of C_{2v} symmetry (**1**, Figure 1a). We show that TRIR remains a powerful technique to detect the localisation of the excitation in molecules without a centre of inversion. Moreover, comparison of **1** with its quasi-linear analogue (**2**, Figure 1a), which was previously found to behave like a centrosymmetric molecule,[7] reveals significant differences in the effect of solvent polarity and structural disorder on the ES-SB dynamics.

The difference in geometry of **1** and **2** can be appreciated by comparing their one- (OPA) and two-photon absorption (TPA) spectra as well as their absorption and emission solvatochromism (Figures 1b,c and S1). Whereas the OPA and TPA spectra of **1** exhibit strong similarities, those of **2** each show a single and distinct band. Lineshape analysis of the spectra of **1** (Figure S2 and Table S1) points to the presence of two transitions, $S_1 \leftarrow S_0$ and $S_2 \leftarrow S_0$, split by $2700\,cm^{-1}$. On the other hand, **2** obeys the mutually exclusive selection rules for OPA and TPA of centrosymmetric molecules.[29] These results can be rationalised with a simple exciton model, where each DA branch is considered as an individual chromophore with a charge-transfer optical transition (Figure 1d).[30,31] Accordingly, the Davydov splitting, $2V$, V being the interbranch coupling energy, is equal to the S_2-S_1 splitting and is predicted to be larger for **2** than for **1**, as observed experimentally. Similarly, the $S_1 \leftarrow S_0$ and $S_2 \leftarrow S_0$ transitions of **1** are predicted to be allowed for both OPA and TPA.

The absorption solvatochromism of **1** is larger than that of **2** (Figure S1). This difference can be attributed to the larger permanent dipole moment of **1**, arising from the 90° angle between its two DA branches. The emission solvatochromism of both dyes is considerably stronger, with the spectrum shifting outside the visible region in solvents with a dielectric constant above ∼6 (Figure 1b). It is about twice as strong for **1** than for **2**, pointing to a higher excited-state dipole moment of **1** in this range of solvent polarity. Plots of the emission energy vs. the orientational polarisation function of the solvent, Δf, point to a possible non-linear behaviour as that expected for ES-SB (Figure S1). However, the range of accessible solvent polarity is too small to draw definitive conclusions.

TRIR spectra recorded in the -C≡C- stretching region upon 400 nm excitation of **1** and **2** in solvents of increasing polarity are illustrated in Figure 2 and Figures S5-S7.

We start with **2**, whose ES-SB dynamics was discussed in detail previously.[7,32] In brief, the TRIR spectra in non-polar solvents are dominated by a single excited-state absorption (ESA) band at $2070\,cm^{-1}$ associated with the antisymmetric -C≡C- stretching mode of the fully delocalised quadrupolar excited state, S_1^{del}. Apart from some initial shift and narrowing due to vibrational and structural relaxation, this

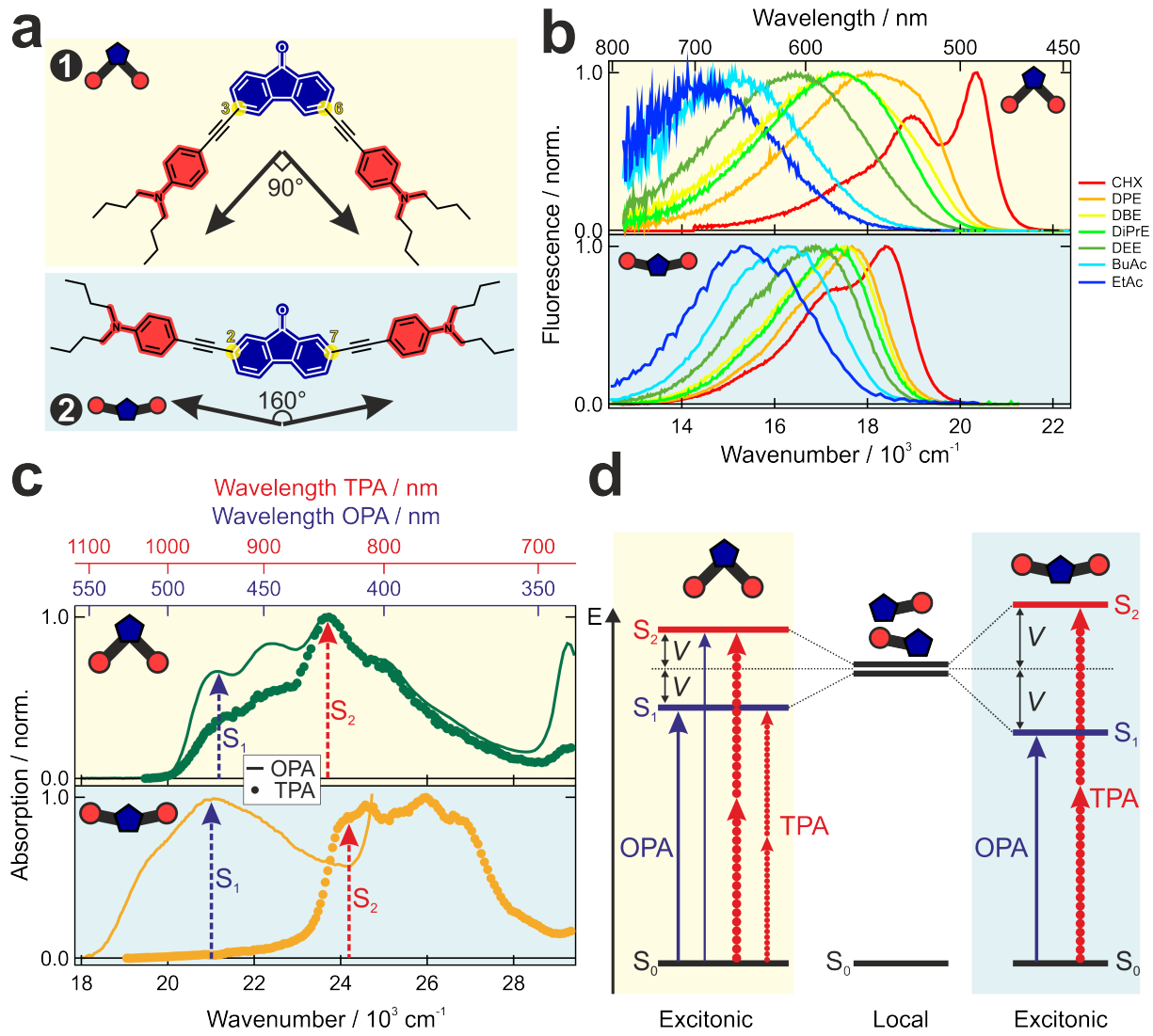

Figure 1: a) Structures of the D-π-A-π-D dyes **1** and **2** with two electron donating aniline fragments (red) and a fluorenone acceptor (dark blue) connected with ethynyl π-spacers. b) Fluorescence solvatochromism of **1** (top) and **2** (bottom). Solvents: CHX – cyclohexane, DPE – dipentyl ether, DBE – dibutyl ether, DiPrE – diisopropyl ether, DEE – diethyl ether, BuAc – butyl acetate, EtAc – ethyl acetate. c) Comparison between one- (OPA, solid line) and two-photon absorption (TPA, markers) spectra of **1** and **2** in cyclohexane. d) Excitonic coupling (V) between the two charge-transfer branches leads to the Davydov splitting of the S_1 and S_2 energy levels. The magnitude of the coupling as well as the selection rules depend on the molecular symmetry: both transitions from S_0 are both OPA and TPA allowed for **1**, whereas for **2** the two transitions are mutually exclusive for OPA and TPA. The thickness of the arrows reflects the oscillator strength of the transition.

band decays on the ns timescale. In weak to medium polar solvents like dibutyl ether (DBE, $\epsilon_s = 3.1$), diethyl ether (DEE, $\epsilon_s = 4.3$) and chloroform ($CHCl_3$, $\epsilon_s = 4.8$), the early spectra exhibit the same band of the S_1^{del} state, but transform in a few ps to a spectrum with two ESA bands, an intense one around 2080 cm^{-1} and a weak one at $\sim$ 2160 cm^{-1}, which remains unchanged during the excited-state lifetime (Figures 2 and S5). This spectrum is due to an 'intermediate' excited state, S_1^I, with a lopsided distribution of the excitation on the two DA branches. Finally in highly polar solvents like benzonitrile (BCN, $\epsilon_s = 25.2$), acetonitrile (ACN, $\epsilon_s = 37.5$) and dimethylsulfoxide (DMSO, $\epsilon_s = 46.7$), the same initial dynamics is observed but the spectrum of the S_1^I state evolves further to a spectrum with a sin-

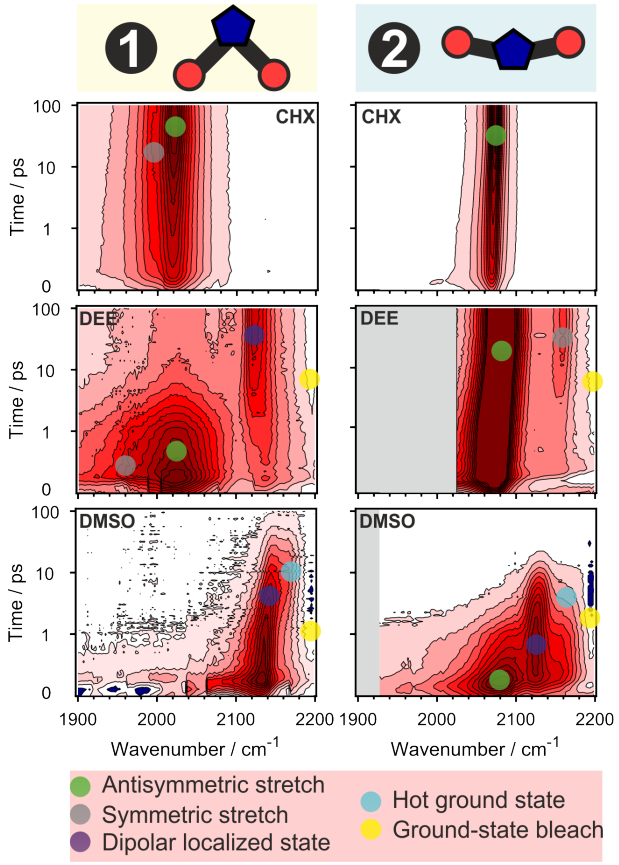

Figure 2: TRIR spectrotemporal maps in the -C≡C- stretch region measured with **1** (left) and **2** (right) in non-polar cyclohexane (CHX), weakly polar diethyl ether (DEE) and highly polar dimethylsulfoxide (DMSO). Vibrational transitions of various states are designated as indicated in the legend. Spectra of **2** were adapted with permission from ref. 7 copyright 2016 American Chemical Society.

gle ESA band at 2130 cm^{-1}. This band was assigned to the -C≡C- stretching mode of the dipolar excited state, S_1^D, with the excitation fully localised on a single DA branch.[7]

The early spectra measured with **1** in CHX present an ESA band around 2020 cm^{-1} with a low-frequency shoulder, which can be assigned to the antisymmetric and the symmetric -C≡C- stretching modes, respectively (Figures 2 and 3). Additionally, the onset of a broad and intense ESA band peaking between 2700 and 3000 cm^{-1}(Figure S6) is visible. This feature, which is absent with **2**, can be attributed to an electronic transition between the two lowest excitonic states of **1**. As discussed previously,[31,33,34] this transition is a characteristic of the delocalised excited state, S_1^{del}. According to the above-mentioned excitonic model (Figure 1d), its energy corresponds to the S_2-S_1 gap, which amounts to 2700 cm^{-1}. Both vibrational and electronic bands of **1** decay concurrently with a ∼800 ps time constant to a residual spectrum consisting of a weak ESA band at 1950 cm^{-1} with a shoulder around 1910 cm^{-1}, which can be ascribed to the two -C≡C- stretching vibrations of **1** in the T_1 state (Figure 3). Like for **2**, the electronic excitation in CHX is distributed evenly on both branches. However, for **1**, this information is mostly deduced from the persistent presence of the mid-IR electronic ESA band of the S_1^{del} state. For **2**, this ESA band should be at higher frequencies, i.e. around 3500 cm^{-1}, as a consequence of a higher interbranch excitonic coupling.

In the weakly polar dibutyl ether, the early spectra measured with **1** exhibit the two bands of the S_1^{del} state as measured in CHX, as well as a new weak ESA band at 2140 cm^{-1} (Figure 3). This band resembles that of the S_1^D state of **2** as well as that measured with a single-branched analogue.[7] Based on this, it is attributed to the fully localised S_1 state of **1**, i.e. the S_1^D state. This assignment is supported by the fact that the subsequent increase of this band with 12 and 240 ps time constants is accompanied by a partial decay of the vibrational and electronic ESA bands of the S_1^{del} state. Afterward, all bands decay concurrently on the ns timescale.

As the solvent polarity is increased further by going to DEE and $CHCl_3$ (Figures 2, 3 and S7), the partial decay of the S_1^{del} bands becomes more pronounced, and the initial and final amplitudes of the S_1^D band are larger. Moreover, the S_1^{del}→S_1^D conversion accelerates considerably and takes place within 15 ps in both solvents. Additionally, the S_1^D band exhibits fast spectral dynamics (Figures S8 and S9), e.g., an approx. 20 cm^{-1} down-shift in 1.8 ps followed by a ∼6 cm^{-1} up-shift in 7 ps in DEE . As discussed in more detail in the Supporting Information (Section S4), this effect is related to the relaxation of the two different subpopulations of the S_1^D state: the first is generated promptly within the instrument response and the other

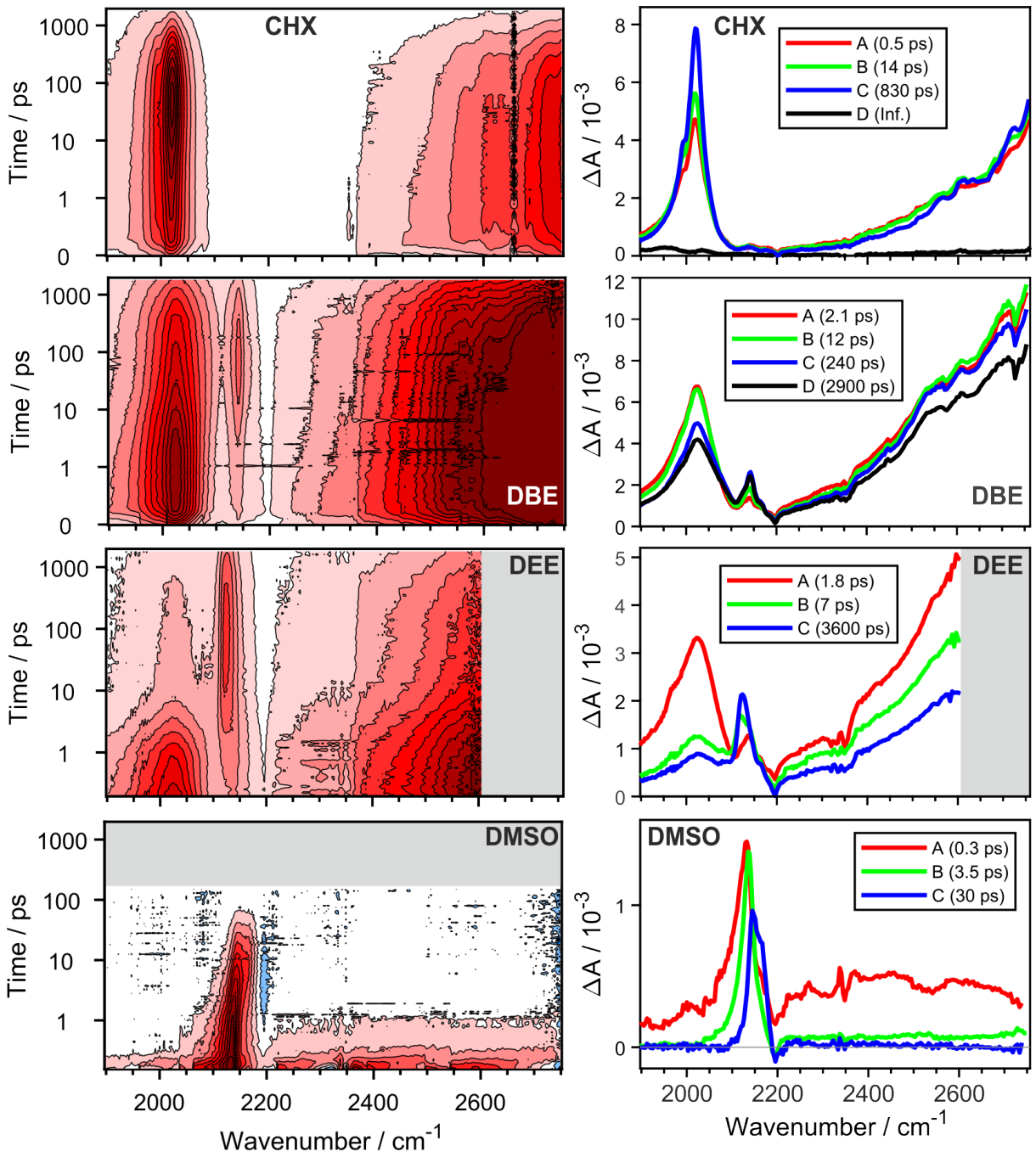

Figure 3: TRIR spectrotemporal maps in non-polar cyclohexane, weakly polar dibutyl and diethyl ethers and highly polar DMSO depicting the -C≡C- vibrational and excitonic $S_2 \leftarrow S_1$ electronic transitions of **1** (left) along with the evolution-associated difference spectra (EADS) and time constants (right) obtained from global analysis assuming sequential A→B→C→(D)→ scheme.

one is formed more slowly from the S_1^{del} state.

Finally, in highly polar solvents like BCN, ACN and DMSO, the spectral features of the S_1^{del} state decay totally within 5 ps and only the S_1^{D} band remains. In turn, this band decays rapidly on multiple timescales, the slowest one decreasing from 110 ps in BCN to 30 and 16 ps in DMSO and ACN, respectively. The evolution-associated difference absorption spectra (EADS), obtained from a global analysis of the TRIR data assuming successive exponential steps (A→B→ . . .), reveal the rise on a few ps of a shoulder on the high-frequency side of the S_1^{D} band (Figure 3 bottom right). Given this timescale and location of this feature on the low-frequency side of the ground-state bleach,

this shoulder is attributed to the vibrationally hot -C≡C- stretching mode of **1** in the electronic ground state. It originates from the ultrafast decay of the S_1^D state in highly polar solvents and the anharmonic coupling of the -C≡C- stretching mode with low-frequency vibrations.[35–37]

These results reveal that ES-SB is not an exclusive property of quadrupolar molecules like **2** and is also operative in two-branched DA dyes of lower symmetry. They also point to major differences in the excited-state dynamics of these two molecules, especially in low to medium polar solvents. Optical excitation of **2** always leads to the population of the delocalised S_1^{del} state, which then evolves further to the S_1^I state. At equilibrium, only the S_1^I state is populated. By contrast, partial population of the S_1^D state of **1** is observed at the earliest time delays. Furthermore, the populations of the S_1^{del} and S_1^D states coexist during the whole excited-state lifetime of **1**. These dissimilarities between **1** and **2** can be understood by considering the potentials along the torsional coordinate around the ethynyl bonds of the DA branches. According to gas-phase quantum-chemical calculations (Section S3), the torsional potential in the electronic ground state is equally shallow for both dyes (Figure 4a). This results in a distribution of dihedral angles between the molecular planes of the D and A sub-units at room temperature, i.e. to torsional disorder, as also reported for other conjugated molecules with ethynyl spacer.[38–45] For **1**, the excited-state torsional potential is similar to that of the ground state, whereas it is about three times as steep for **2**. This effect originates from the conjugation between the fluorenone core and the ethynyl branches in the excited state, which is larger for substitution in 2,7- than 3,6- positions.

This difference in the excited-state potentials has two important consequences. First, torsional disorder should still be present in the excited state of **1**, whereas it should be strongly reduced for **2**. In other words, the conformational ensemble of molecules **1** remains mostly unchanged upon excitation, whereas molecules

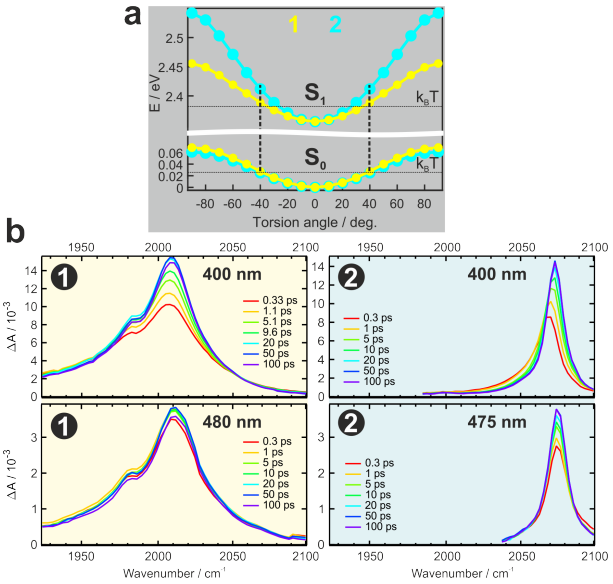

Figure 4: a) Gas-phase calculations (CAM-B3LYP/6-31G(d,p)) of the energy of the ground (bottom) and Franck-Condon S_1 states (top) of **1** (yellow) and **2** (cyan) along the torsional coordinate, defined as the dihedral angle between the fluorenone and one of the aniline planes. The excited-state energy of **2** was upshifted by 0.248 eV for the sake of comparison. Accessible thermal energy (k_BT) at room temperature is shown as a horizontal dashed line for both states. b) TRIR spectra recorded with **1** (left) and **2** (right) in cyclohexane upon 400 nm and 480 nm excitation.

2 planarise.

Second, the S_1- S_0 gap is independent of the torsional angle for **1** but not for **2**. Therefore, photoselection of sub-populations with different amounts of disorder should be possible with **2**,[41–45] but not with **1**. To check these predictions, TRIR measurements with both dyes were carried out in CHX using various excitation wavelengths. As illustrated in Figures 4 and S10, the TRIR spectra recorded with **1** essentially do not depend on whether excitation is done at the red edge of the $S_1 \leftarrow S_0$ band or at the centre of the $S_2 \leftarrow S_0$ band. No signature of the S_1^D band can be observed in CHX regardless of the excitation wavelength (Figure S10). The initial intensity rise and narrowing of the band can be attributed to the dissipation of the excess excitation energy via vibrational relaxation. In the case of **2**, the -C≡C- ESA

band exhibits an initial blue shift and narrowing upon excitation in the $S_2 \leftarrow S_0$ band, while it remains unchanged upon red-edge $S_1 \leftarrow S_0$ excitation. The same behaviour was reported for another linear DAD dye with ethynyl spacers.[42] The initial shift and narrowing observed with excess excitation energy was found to originate from the planarisation of distorted molecules, additionally to vibrational relaxation. This previous study also revealed that, because of this fast planarisation, torsional disorder does not influence the ES-SB dynamics, which is mostly driven by solvation.[42]

Based on this, the TRIR dynamics observed with **1** can be explained as follows. Independently of the wavelength, photoexcitation of **1** projects the ground-state torsional disorder onto the S_1 state. According to gas-phase quantum-chemical calculations, the amplitude of the HOMO, which is involved in the $S_1 \leftarrow S_0$ transition, is delocalised over the whole molecule, but it is larger on the less distorted branch (Figure S4). Therefore, in non-polar solvents, excitation is delocalised on both branches, possibly unevenly for the most distorted molecules. However, considering the amplitude of the disorder at room temperature (Figure 4a), the asymmetry should be rather weak. In any case, full localisation in non polar solvent would cause a loss of interbranch excitonic coupling, and should thus be an energetically uphill process.[28]

Upon increasing solvent polarity, localisation of the excitation becomes energetically more favourable as the gain of solvation energy compensates for the loss of excitonic coupling. In weak to medium polar solvents, occurrence of ES-SB depends on the extent of distortion (Figure 5). For the most distorted subpopulation, the electronic distribution should be sufficiently asymmetric for localisation to occur with inertial solvent reorganisation only. This can account for the observation of the S_1^D band at the earliest time delays. On the other hand, for the subpopulation of the less distorted molecules, excitation remains delocalised and the localisation takes place more slowly via diffusive solvent motion. The energy difference between the S_1^{del} and S_1^D states should be small enough for their populations to be in equilibrium. The presence of this equilibrium points to the existence of a barrier between these two states. Given that localisation is favoured by structural distortion and the asymmetry in the solvent field, this barrier involves most probably torsional and solvent motion.

As solvent polarity increases, the S_1^D state becomes more stable relative to the S_1^{del} state, less distortion is required for localisation, and the equilibrium is shifted toward this state. Finally, in benzonitrile and more polar solvents, the gain in solvation energy upon localisation is large enough for only the S_1^D state to be populated.

Although ES-SB is operative with both linear and right-angled DAD dyes in polar media, the delocalised state is only observed in non-polar solvents with **2**, whereas it is still populated in medium polar environments with **1**. This difference can be explained by considering the energetics of the localisation. As mentioned above, for localisation to take place, the loss of interbranch coupling has to be compensated by a gain in solvation energy.[23,28] In a given solvent, this gain is significantly larger for a linear molecule, because localisation leads to a transition from a purely quadrupolar to a dipolar state. By contrast, molecule **1** has already a strong dipolar character in the delocalised state, and therefore the difference in solvation energy between the S_1^{del} and S_1^D state is markedly smaller than for dye **2**. In other words, more polar solvents are required to make this difference of solvation energy larger than the interbranch coupling.

To sum up, we could show that ES-SB can be detected using TRIR spectroscopy with a DAD dye lacking a centre of inversion. Two main differences were observed between the linear and the right-angle geometries. The first is that the torsional disorder that is present for both dyes in the ground state is preserved in the excited state for the right-angled dye. This leads to the coexistence of subpopulations with delocalised and localised excitation in equilib-

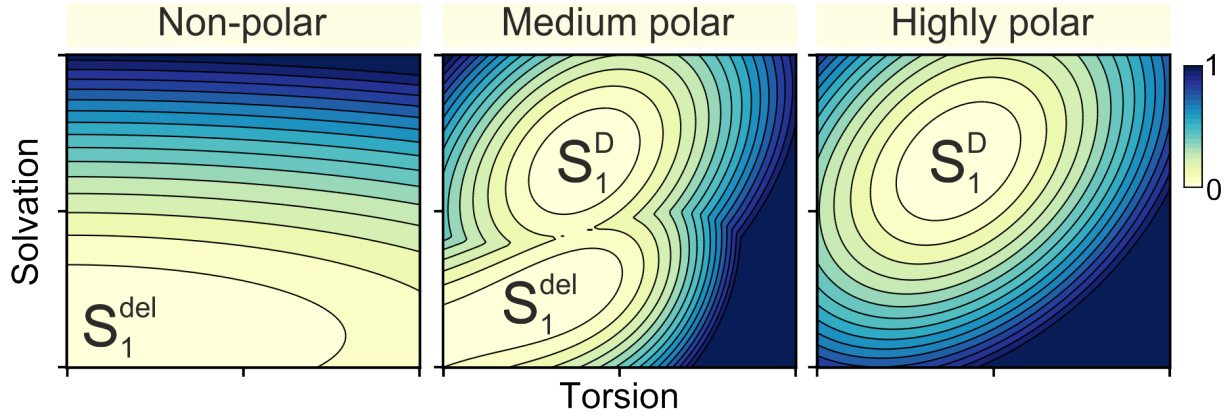

Figure 5: Schematic depiction of the energy of the S_1 state of **1** in non-polar (left), medium-polar (middle) and highly-polar (right) solvents along torsional and solvation coordinates. The latter coordinate also reflects the extent of localisation of the excitation. In non-polar solvents, symmetry-preserved delocalised state, S_1^{del}, is favoured, while localised fully symmetry-broken state, S_1^{D}, dominates in highly polar media. In medium polar solvents, both states are in equilibrium pointing to a low energy barrier between them. Note the correlation between the torsional disorder coordinate and localisation (solvation coordinate) in this case.

rium in weakly to medium polar solvents. The second is that the driving force for the localisation of the excitation is smaller than for a centrosymmetric dye, because the gain in solvation energy is weaker, due to dye having a permanent dipole moment independently of whether excitation is localised or not. Such knowledge should certainly be useful for better controlling the distribution of electronic excitation in large multibranched conjugated molecular architectures.

Acknowledgement Financial support from the Swiss National Science Foundation (grants 200020-184607 (E.V.), PZ00P2_201996 (B.D.) and the University of Geneva is acknowledged. B.D. thanks Prof. Peter Hamm (University of Zurich) for generously hosting and supporting his research group. The computations were performed at the University of Geneva using Baobab HPC service.

Supporting Information Available

Experimental details, additional results: stationary spectroscopy, time-resolved IR data, quantum-chemical calculations. The data can be downloaded from https://doi.org/10.26037/yareta:hhhyrnxd3zbeho74z33s4evra4

References

(1) Amthor, S.; Lambert, C.; Dümmler, S.; Fischer, I.; Schelter, J. Excited Mixed-Valence States of Symmetrical Donor-Acceptor-Donor π Systems. *J. Phys. Chem. A* **2006**, *110*, 5204–5214.

(2) Terenziani, F.; Painelli, A.; Katan, C.; Charlot, M.; Blanchard-Desce, M. Charge Instability in Quadrupolar Chromophores: Symmetry Breaking and Solvatochromism. *J. Am. Chem. Soc.* **2006**, *128*, 15742–15755.

(3) Sissa, C.; Painelli, A.; Blanchard-Desce, M.; Terenziani, F. Fluorescence Anisotropy Spectra Disclose the Role of Disorder in Optical Spectra of Branched Intramolecular-Charge-Transfer Molecules. *J. Phys. Chem. B* **2011**, *115*, 7009–7020.

(4) Carlotti, B.; Benassi, E.; Spalletti, A.; Fortuna, C. G.; Elisei, F.; Barone, V. Photoinduced Symmetry-Breaking Intramolecular Charge Transfer in a Quadrupolar Pyridinium Derivative.

Phys. Chem. Chem. Phys. **2014**, *16*, 13984–13994.

(5) Rebane, A.; Drobizhev, M.; Makarov, N. S.; Wicks, G.; Wnuk, P.; Stepanenko, Y.; Haley, J. E.; Krein, D. M.; Fore, J. L.; Burke, A. R. et al. Symmetry Breaking in Platinum Acetylide Chromophores Studied by Femtosecond Two-Photon Absorption Spectroscopy. *J. Phys. Chem. A* **2014**, *118*, 3749–3759.

(6) Carlotti, B.; Benassi, E.; Fortuna, C. G.; Barone, V.; Spalletti, A.; Elisei, F. Efficient Excited-State Symmetry Breaking in a Cationic Quadrupolar System Bearing Diphenylamino Donors. *ChemPhysChem* **2016**, *17*, 136–146.

(7) Dereka, B.; Rosspeintner, A.; Li, Z.; Liska, R.; Vauthey, E. Direct Visualization of Excited-State Symmetry Breaking Using Ultrafast Time-Resolved Infrared Spectroscopy. *J. Am. Chem. Soc.* **2016**, *138*, 4643–4649.

(8) Dereka, B.; Rosspeintner, A.; Krzeszewski, M.; Gryko, D. T.; Vauthey, E. Symmetry-Breaking Charge Transfer and Hydrogen Bonding: Toward Asymmetrical Photochemistry. *Angew. Chem. Int. Ed.* **2016**, *55*, 15624–15628.

(9) Dozova, N.; Ventelon, L.; Clermont, G.; Blanchard-Desce, M.; Plaza, P. Excited-State Symmetry Breaking of Linear Quadrupolar Chromophores: A Transient Absorption Study. *Chem. Phys. Lett.* **2016**, *664*, 56–62.

(10) Lee, S.; Kim, D. Symmetry-Dependent Intramolecular Charge Transfer Dynamics of Pyrene Derivatives Investigated by Two-Photon Excitation. *J. Phys. Chem. A* **2016**, *120*, 9217–9223.

(11) Beckwith, J. S.; Rosspeintner, A.; Licari, G.; Lunzer, M.; Holzer, B.; Fröhlich, J.; Vauthey, E. Specific Monitoring of Excited-State Symmetry Breaking by Femtosecond Broadband Fluorescence Upconversion Spectroscopy. *J. Phys. Chem. Lett.* **2017**, *8*, 5878–5883.

(12) Cooper, T. M.; Haley, J. E.; Krein, D. M.; Burke, A. R.; Slagle, J. E.; Mikhailov, A.; Rebane, A. Two-Photon Spectroscopy of a Series of Platinum Acetylides: Conformation-Induced Ground-State Symmetry Breaking. *J. Phys. Chem. A* **2017**, *121*, 5442–5449.

(13) Dereka, B.; Rosspeintner, A.; Stężycki, R.; Ruckebusch, C.; Gryko, D. T.; Vauthey, E. Excited-State Symmetry Breaking in a Quadrupolar Molecule Visualized in Time and Space. *J. Phys. Chem. Lett.* **2017**, *8*, 6029–6034.

(14) Łukasiewicz, L. G.; Ryu, H. G.; Mikhaylov, A.; Azarias, C.; Banasiewicz, M.; Kozankiewicz, B.; Ahn, K. H.; Jacquemin, D.; Rebane, A.; Gryko, D. T. Symmetry Breaking in Pyrrolo[3,2-b]pyrroles: Synthesis, Solvatofluorochromism and Two-photon Absorption. *Chem. Asian J.* **2017**, *12*, 1736–1748.

(15) Sonoda, Y. Absorption and Fluorescence Solvatochromic Behaviors of Centrosymmetric D-π-D Molecules with TTF/Dimethylamino Electron Donors and Polyenic π-Bridge. *J. Lumin.* **2017**, *187*, 352–359.

(16) Kurhuzenkau, S. A.; Colon Gomez, M. Y.; Belfield, K. D.; Shaydyuk, Y. O.; Hagan, D. J.; Van Stryland, E. W.; Sissa, C.; Bondar, M. V.; Painelli, A. Electronic Nature of Nonlinear Optical Properties of a Symmetrical Two-Photon Absorbing Fluorene Derivative: Experimental Study and Theoretical Modeling. *J. Phys. Chem. C* **2018**, *122*, 5664–5672.

(17) Bardi, B.; Krzeszewski, M.; Gryko, D. T.; Painelli, A.; Terenziani, F. Excited-State Symmetry Breaking in an Aza-Nanographene Dye. *Chem. Eur. J.* **2019**, *25*, 13930–13938.

(18) Chung, H. Y.; Oh, J.; Park, J.-H.; Cho, I.; Yoon, W. S.; Kwon, J. E.; Kim, D.; Park, S. Y. Spectroscopic Studies on Intramolecular Charge-Transfer Characteristics in Small-Molecule Organic Solar Cell Donors: A Case Study on ADA and DAD Triad Donors. *J. Phys. Chem. C* **2020**, *124*, 18502–18512.

(19) Łukasiewicz, L. G.; Rammo, M.; Stark, C.; Krzeszewski, M.; Jacquemin, D.; Rebane, A.; Gryko, D. T. Ground- and Excited-State Symmetry Breaking and Solvatofluorochromism in Centrosymmetric Pyrrolo[3,2-b]pyrroles Possessing two Nitro Groups. *ChemPhotoChem* **2020**, *4*.

(20) Niu, X.; Kuang, Z.; Planells, M.; Guo, Y.; Robertson, N.; Xia, A. Electron-Donating Strength Dependent Symmetry Breaking Charge Transfer Dynamics of Quadrupolar Molecules. *Phys. Chem. Chem. Phys.* **2020**, *22*, 15743–15750.

(21) Bondarev, S. L.; Raichenok, T. F.; Tikhomirov, S. A.; Kozlov, N. G.; Mikhailova, T. V.; Ivanov, A. I. Symmetry Breaking in an Excited Quadrupolar Acridine-Dione Derivative Driven by Hydrogen Bonding. *J. Phys. Chem. B* **2021**, *125*, 8117–8124.

(22) Cesaretti, A.; Spalletti, A.; Elisei, F.; Foggi, P.; Germani, R.; Fortuna, C. G.; Carlotti, B. The Role of Twisting in Driving Excited-State Symmetry Breaking and Enhanced Two-Photon Absorption in Quadrupolar Cationic Pyridinium Derivatives. *Phys. Chem. Chem. Phys.* **2021**, *23*, 16739–16753.

(23) Szakács, Z.; Glöcklhofer, F.; Plasser, F.; Vauthey, E. Excited-State Symmetry Breaking in 9,10-Dicyanoanthracene-Based Quadrupolar Molecules: the Effect of Donor–Acceptor Branch Length. *Phys. Chem. Chem. Phys.* **2021**, *23*, 15150–15158.

(24) Usta, H.; Cosut, B.; Alkan, F. Understanding and Tailoring Excited State Properties in Solution-Processable Oligo(p-phenyleneethynylene)s: Highly Fluorescent Hybridized Local and Charge Transfer Character via Experiment and Theory. *J. Phys. Chem. B* **2021**, *125*, 11717–11731.

(25) Wei, Z.; Sharma, S.; Philip, A. M.; Sengupta, S.; Grozema, F. C. Excited State Dynamics of BODIPY-Based Acceptor–Donor–Acceptor Systems: a Combined Experimental and Computational Study. *Phys. Chem. Chem. Phys.* **2021**, *23*, 8900–8907.

(26) Fakis, M.; Petropoulos, V.; Hrobárik, P.; Nociarová, J.; Osuský, P.; Maiuri, M.; Cerullo, G. Exploring Solvent and Substituent Effects on the Excited State Dynamics and Symmetry Breaking of Quadrupolar Triarylamine End-Capped Benzothiazole Chromophores by Femtosecond Spectroscopy. *J. Phys. Chem. B* **2022**, *126*, 8532–8543.

(27) Guo, S.; Liu, W.; Wu, Y.; Sun, J.; Li, J.; Jiang, H.; Zhang, M.; Wang, S.; Liu, Z.; Wang, L. et al. Distinctive Excited State Symmetry Breaking Dynamics in Typical Donor–Acceptor–Donor Fluorophore: Strong Photoluminescence and Ultrafast Charge Separation from a Partial Charge Transfer State. *J. Phys. Chem. Lett.* **2022**, *13*, 7547–7552.

(28) Verma, P.; Tasior, M.; Roy, P.; Meech, S. R.; Gryko, D. T.; Vauthey, E. Excited-State Symmetry Breaking in Quadrupolar Pull–Push–Pull Molecules: Dicyanovinyl vs. Cyanophenyl Acceptors. *Phys. Chem. Chem. Phys.* **2023**, *25*, 22689–22699.

(29) Pawlicki, M.; Collins, H.; Denning, R.; Anderson, H. Two-Photon Absorption and the Design of Two-Photon Dyes. *Angew. Chem. Int. Ed. 48*, 3244–3266.

(30) Kasha, M.; Rawls, H. R.; El-Bayoumi, M. A. The Exciton Model

in Molecular Spectroscopy. *Pure Appl. Chem.* **1965**, *11*, 371–392.

(31) Vauthey, E. Watching Excited-State Symmetry Breaking in Multibranched Push–Pull Molecules. *J. Phys. Chem. Lett.* **2022**, *13*, 2064–2071.

(32) Balanikas, E.; Reymond-Joubin, M.; Vauthey, E. Excited-State Symmetry Breaking in Solvent Mixtures. *The Journal of Physical Chemistry Letters* **2024**, *15*, 2447–2452.

(33) Dereka, B.; Svechkarev, D.; Rosspeintner, A.; Aster, A.; Lunzer, M.; Liska, R.; Mohs, A. M.; Vauthey, E. Solvent Tuning of Photochemistry upon Excited-State Symmetry Breaking. *Nature Commun.* **2020**, *11*, 1925.

(34) Ivanov, A. I. Electric Dipole Flip in a Quadrupolar Molecule with Broken Symmetry upon Excited State Absorption. *J. Chem. Phys.* **2023**, *159*, 054302.

(35) Hamm, P.; Ohline, S. M.; Zinth, W. Vibrational Cooling after Ultrafast Photoisomerization of Azobenzene Measured by Femtosecond Infrared Spectroscopy. *J. Chem. Phys.* **1997**, *106*, 519–529.

(36) Hirai, S.; Banno, M.; Ohta, K.; Palit, D. K.; Tominaga, K. Vibrational Dynamics of the CO Stretching Mode of 9-Fluorenone in Alcohol Aolution. *Chem. Phys. Lett.* **2007**, *450*, 44–48.

(37) Zhang, Y.; Improta, R.; Kohler, B. Mode-Specific Vibrational Relaxation of Photoexcited Guanosine 5'-Monophosphate and its Acid Form: a Femtosecond Broadband Mid-IR Transient Absorption and Theoretical Study. *Phys. Chem. Chem. Phys.* **2014**, *16*, 1487–1499.

(38) Sluch, M. I.; Godt, A.; Bunz, U. H. F.; Berg, M. A. Excited-State Dynamics of Oligo(p-phenyleneethynylene): Quadratic Coupling and Torsional Motions. *J. Am. Chem. Soc.* **2001**, *123*, 6447–6448.

(39) Magyar, R. J.; Tretiak, S.; Gao, Y.; Wang, H.-L.; Shreve, A. P. A Joint Theoretical and Experimental Study of Phenylene–Acetylene Molecular Wires. *Chem. Phys. Lett.* **2005**, *401*, 149–156.

(40) Greaves, S. J.; Flynn, E. L.; Futcher, E. L.; Wrede, E.; Lydon, D. P.; Low, P. J.; Rutter, S. R.; Beeby, A. Cavity Ring-Down Spectroscopy of the Torsional Motions of 1,4-Bis(phenylethynyl)benzene. *J. Phys. Chem. A* **2006**, *110*, 2114–2121.

(41) Roy, K.; Kayal, S.; Ravi Kumar, V.; Beeby, A.; Ariese, F.; Umapathy, S. Understanding Ultrafast Dynamics of Conformation Specific Photo-Excitation: A Femtosecond Transient Absorption and Ultrafast Raman Loss Study. *J. Phys. Chem. A* **2017**, *121*, 6538–6546.

(42) Soederberg, M.; Dereka, B.; Marrocchi, A.; Carlotti, B.; Vauthey, E. Ground-state Structural Disorder and Excited-state Symmetry Breaking in a Quadrupolar Molecule. *J. Phys. Chem. Lett.* **2019**, *10*, 2944–2948.

(43) Fureraj, I.; Budkina, D. S.; Vauthey, E. Torsional Disorder and Planarization Dynamics: 9,10-Bis(phenylethynyl)anthracene as a Case Study. *Phys. Chem. Chem. Phys.* **2022**, *24*, 25979–25989.

(44) Ringström, R.; Edhborg, F.; Schroeder, Z. W.; Chen, L.; Ferguson, M. J.; Tykwinski, R. R.; Albinsson, B. Molecular Rotational Conformation Controls the Rate of Singlet Fission and Triplet Decay in Pentacene Dimers. *Chem. Sci.* **2022**, *13*, 4944–4954.

(45) Mendis, K. C.; Li, X.; Valdiviezo, J.; Banziger, S. D.; Zhang, P.; Ren, T.; Beratan, D. N.; Rubtsov, I. V. Electron Transfer Rate Modulation with Mid-IR in Butadiyne-Bridged Donor–Bridge–Acceptor Compounds. *Phys. Chem. Chem. Phys.* **2024**, *26*, 1819–1828.